

Characterisation of carbon nanotubes decorated with platinum nanoparticles

M. Pawlyta*, D. Łukowiec, A.D. Dobrzańska-Danikiewicz

Silesian University of Technology,
ul. Konarskiego 18a, 44-100 Gliwice, Poland

* Corresponding e-mail address: mirosława.pawlyta@polsl.pl

Received 11.06.2012; published in revised form 01.08.2012

Materials

ABSTRACT

Purpose: In presented work results of synthesis of carbon nanotubes decorated with platinum nanoparticles by organic colloidal process as an example of direct formation of nanoparticles onto CNTs are reported.

Design/methodology/approach: Powder XRD and transmission electron microscopy were used for characterisation of the morphology of composite as well as the distribution of nanocrystals on the CNTs surfaces.

Findings: TEM results confirm that CNT were homogeneous and clean, without any admixtures and carbon deposits. High efficiency of covering carbon nanotubes (without aggregation) by platinum nanoparticles by organic colloidal process was confirmed. Observed particles appear to have a narrow size distribution. HAADF images confirm homogeneous covering of carbon nanotubes. Large clusters as well as empty fragments were not observed.

Research limitations/implications: Some properties of materials in nanoscale strongly depend on size and are significantly changed if that size is smaller than 100 nm. Majority of these effects were no described and explained so far, what is mainly follows that image the object at nanoscale is difficult.

Practical implications: Carbon nanotubes decorated with platinum and other precious metal nanoparticles can be characterised with atomic resolution by scanning transmission electron microscopy.

Originality/value: Results of characterisation of raw carbon nanotubes as well as carbon nanotubes decorated with platinum nanoparticles were demonstrated in this work.

Keywords: Nanomaterials; Carbon nanotubes; Platinum nanoparticles; Nanocomposites

Reference to this paper should be given in the following way:

M. Pawlyta, D. Łukowiec, A.D. Dobrzańska-Danikiewicz, Characterisation of carbon nanotubes decorated with platinum nanoparticles, Journal of Achievements in Materials and Manufacturing Engineering 53/2 (2012) 67-75.

1. Introduction

Carbon nanotubes (CNT) are nanometric structures formed from rolled up graphene layers. Their diameters are from fraction to a few dozen nanometers, while their length can achieve a few micrometers. Because of electronic, mechanical, chemical, magnetic and optical properties carbon nanotubes are currently a subject of very intensive scientific research [5]. Authorities indicate four main CNT application areas, which are: electron

technology (flat displays FED, cathodes at high-power microwave amplifiers, electron emitters in electron microscopes), microelectronics (transistors FED, hypothetical quantum computers), nanocomposites (reinforced with carbon nanotubes) and electrochemistry (energy storage, lithium ion batteries, supercapacitors, nanosensors) [6,7].

Potential applications of carbon nanotubes can be exploited on a large scale only if CNTs are controllably assembled into more sophisticated and hierarchical architectures as well as joined with other materials. For that reason it is extremely important to

study covering carbon nanotubes surface with metal and semiconductor nanoparticles (NPs). Nanocomposites (CNT-NPs), obtained as result of that process may be a valuable material because of combination of unique physical and chemical properties of its components [5,8]. Both components are characterised by large specific surface area and high value of electric conductivity. More over carbon nanotubes are light (its density is ca 1.33-1.40 g/cm³), elastic and resistant to bending, stretching and twining. Bonding between carbon atoms in carbon nanotubes are strong (stronger than in diamond), and simultaneously theirs surface is chemically and thermally resistant. It was confirmed [9,10] that carbon nanotubes conductivity changed as result of the interaction with molecules of many chemical substances, both liquids and gases. That effect is even more distinct after covering the carbon nanotubes surface with noble metals (Au, Pt, Pd, Rh) [11,12].

An importance and range of sensor application dynamically increase. Sensors can be used when analysed signal can't be recorded directly by human senses or when it works as a part of equipment automatically reacting on new signal and also when it is desirable that signal is recorded without human activity. Chemical sensor operations consisting in of taking advantage of phenomena which occur on the phase border: solid - gas or solid - liquid. As a result of the influence of the phase including analysed substance with active surface of the sensor chemical bonds between molecules of analysed substance and adsorbant material are formed. As a result of that process the concentration of the charge carrier is changed, causing a change in the surface conductivity. This phenomena is connected only with very thin, superficial layer of the material. The increasing ratio of surface to volume causes the sensor to be more sensitive to contact with gases or liquids. For that reason it is justified to apply materials with large surface areas for sensor's construction, like carbon nanotubes, especially coated with metal nanocrystals [12]. An advantages of sensors with carbon nanotubes coated with metal nanocrystals are small size and possibility to detect multiple gases at the same time.

The aim of the researches connected with carbon nanotubes application is to use of theirs electrical, mechanical and thermal properties for construction of sensors with better parameters (sensitivity, selectivity, speed, accuracy). The second intention is to obtain sensors with properties which make possible to apply them at new conditions [11]. An example is application of sensors with carbon nanotubes as active elements as implant which control health condition (in that case the size is a critical factor) and at motor industry for precise monitoring of work conditions at particular part of engine (here apart from size thermal stability is also very important). Hybrid materials including metal nanocrystals and carbon nanotubes have many medical applications. Examples are cholesterol [13] or glucose sensors [14]. Such sensors can be also applied at food industry (for monitoring of food storage and toxic substances detection), agriculture (for monitoring of conditions at greenhouses), environmental protection (at atmosphere pollution researches, connected with CO₂, NO_x and CH₄ emission) and at domestic and industrial gas installations (for assessment of their tightness and for detection of hazardous substances). Sensors miniaturization results in decreasing of their weight, energy consumption and production costs.

Essential for CNT-NPs applications is control of effectivity and homogeneity of the covering of nanoparticles on the surface of

the carbon nanotubes. Crucial for solving that problem is explanation of the mechanism of forming obtained nanostructures and describing the type and determination the amount of defects which are formed during covering process. The aim of the conducted research is to develop the methodology of forming nanocomposites including nanocrystals with precisely defined size, shape, chemical composition and type of sitting on the surface of the carbon nanotubes. Dissemination of effective procedures of covering carbon nanotubes by metals nanoparticles may results in significant progress in researches connected with optoelectronic, medicine, accumulation and conversion of energy, where many prospective applications of described hybrid materials could be indicated [15-19]. Difficulty in access to nanocomposite materials obtained as result of covering carbon nanotubes by metal nanoparticles is now the main barrier of the progress in researches connected with its application at these activity areas.

In [11] numerous examples of sensor applications in medicine, environmental protection, food industry, agriculture and industry were presented. Review of the substances which can be detected and registered by that type of sensors were performed. The most important examples are: NH₃, CO₂, O₂, NO₂, CH₄, H₂, N₂, Ar, ethanol, CO, NO, glucose, H₂O₂, SF₆, DNA and many others.

Platinum is an important raw material with many applications, for example as catalyst for CO oxidation in catalytic converters and for fuel cell technology [8]. For many years efforts have been made to increase effectivity of its use. One of the method is to produce platinum nanocrystals. Size of the nanocrystals is connected with specific surface area - decreasing of the average nanocrystal diameter results in increase of value of specific surface area. A second factor which motivates nanomaterial investigations, including platinum, is that some properties of materials in nanoscale strongly depend on size and are significantly changed if that size is smaller than 100 nm. Because of nanometric size image such nanostructures and test their properties is a challenge. In last year the unusual progress was achieved at that area. Techniques which make it possible to obtain atomic resolution and could be used in this research were developed and disseminated. The aim of this paper was to structure and morphology investigation with nano resolution, using mainly transmission electron microscopy.

2. Experimental

2.1. Materials for investigations

Organic colloidal process of deposition of Pt nanoparticles was described in earlier works [1-4]. Tested procedure of Pt nanoparticles deposition turned out to be highly effective and gives possibility of the coating of Pt nanoparticles onto CNTs, without aggregation of these particles. To deposit Pt nanoparticles on the functionalized CNTs, 148 mg pretreated CNTs were dispersed into 15 mL ethylene glycol by ultrasonic vibration for 0.5 h. The obtained suspension was mixed with 5 mL of acetone with continuous stirring. Afterwards 5 mL H₂PtCl₆ solution (0.0386 M) and 0.114 g sodium citrate were added and the pH

value of the obtained suspension was adjusted to 8 by addition of 5% NaOH solution. After stirring for half an hour and heating in oil bath at 150°C for 8 h the obtained material was washed with water for 3 times and finally dried at 70°C.

2.2. Platinum structure

Platinum unit cell is presented in Fig. 1. Data which describe that unit originate from Crystallography Open Database (file 9008480.cif) [22]. Platinum crystallize in cubic crystal system, the length of basic vector $a=3.9231\text{Å}$, volume of unit cell 60.379Å^3 ; Hermann-Mauguin symmetry space group: F m $\bar{3}$ m; Hall symmetry space group -F 4 2 3).

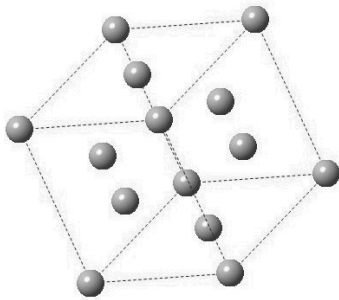


Fig. 1. Platinum unit cell

2.3. XRD investigations

The crystal structure of the Pt nanoparticles supported on CNTs was determined by powder XRD diffractometer (Panalytical X'Pert Pro, Co K_{α} radiation, $\lambda = 1.54050\text{Å}$). For the determination of the position of the diffraction peaks in XRD pattern curve fitting was performed with the software program Fityk (Levenberg-Marquardt algorithm) [23]. The goodness-of-fit was indicated by the residuals between the calculated fit curve and the observed spectrum. Determined positions of the diffraction peaks in XRD pattern were compared with JCPDS data sets to obtain crystallographic parameters (Tab. 1).

Table 1.

The crystallographic parameters of the chemical components (the Bragg angle 2θ for for Cu K_{α} radiation)

Chemical name	2θ , degrees	d_{hkl} , Å	hkl
Platinum JCPDS 87-0647	40.246	2.2389	(111)
	46.814	1.9390	(200)
	68.362	1.3710	(220)
	82.413	1.1692	(311)
Graphite JCPDS 75-1621	26.228	3.3950	(002)

For determination of crystallite size with diameter less than 100 nm methods based on analysis of profile of diffraction lines can be applied. In our work Williamson-Hall's method was used. First the mathematical formula of the function which describe the

diffraction lines is assumed. For Pt peaks Gauss function was chosen ($y=\exp(-ax^2)$). Next the experimental results are approximated by these functions. Width of the reflections can be determined as integral breadth or full width at half maximum FWHM. Physical factors (crystallite size, lattice strain) as well as apparatus factors influence on X-ray diffraction line broadening and should be took into account. It can be assumed that diffraction line broadening resulting from small crystallite size β_K can be described by the Debye-Scherrer formula:

$$D = \frac{K\lambda}{\beta_K \cos(\theta)}, \quad (1)$$

in which D is the crystallite size, λ the wavelength of the X-ray radiation, K is usually taken as 0.9, 2θ is the Bragg angle of the Pt peak, and β_K is the line width at half-maximum height, after subtraction of equipment broadening. Line broadening resulting from lattice strain β_Z is described by Taylor formula:

$$\beta_Z = 4e \tan \theta, \quad (2)$$

where e is lattice strain. Total broadening β is a sum of both broadenings. In such conditions $\beta=B-b$, where b is an apparatus broadening, experimentally determined for standard (Si) sample. In our investigations $b=0.23^\circ$. Relationship between crystallite size, line broadenings and Bragg angles are described as:

$$\beta^2 \cos^2 \theta = (\lambda / D)^2 + 16e^2 \sin^2 \theta, \quad (3)$$

and make possible to determine crystallite size.

2.4. TEM investigations

Because of precision, efficiency, cost and representativity of obtained results, X-ray diffraction (XRD) is the most frequently method for nanomaterials investigations. Simultaneously powder XRD diffraction with reference to nanomaterials characterisation has three crucial disadvantages:

- phases with weight content less than 2% are not identified,
- identification is not unambiguous,
- averaged information are obtained from all analysed volume.

Limitations connected with XRD detection limit can be exceed by electron microscopy, especially transmission electron microscopy TEM. A conventional TEM (CTEM) always consists of similar basic components: electron emitter, condenser lens system, specimen, objective lens, intermediate lens, projector lens system and fluorescent screen or TV/CCD camera. The electron beam is strongly accelerated up to typical value between 80 and 300 kV. Condenser lens system controls the demagnification of the source and size of the spot at the specimen and beam convergence. The main electromagnetic objective lens forms the first intermediate, real-space projection image of the illuminated specimen area as well as corresponding reciprocal space diffraction pattern. The image or diffraction pattern is magnified by a series of projector lenses. Final magnification may exceed value equal 1000 000 times. A CTEM images consists of

combination of mass-thickness contrast, diffraction contrast and at higher magnifications phase contrast. Scanning Transmission Electron Microscope (STEM) consist with the same basic components - both instruments differ principally in the way they address the specimen. The conventional TEM is a wide beam technique, while STEM deploys a fine focused beam which scans a surface of the specimen and scattered signal is analyzed. High-Angle-Dark-Field-Detector (HAADF) almost entirely eliminates diffraction contrast and has become the most widely used imaging method in STEM, because of its efficiency and the ease of interpretation of the obtained images. Their great advantage for imaging and analysis is that HAADF images are usually insensitive to structure and orientation but strongly dependant on atomic number. As platinum and carbon have significantly different atomic numbers (for carbon $Z=6$, for platinum $Z=78$), that method was expected to be very useful for carbon nanotubes covered by platinum nanoparticles characterisation [21,21].

The crystal structure and morphology of the Pt nanoparticles supported on CNTs was determined by electron microscopy in high resolution transmission electron microscope S/TEM TITAN 80-300 (FEI Company) with field-emission gun (FEG), bright field, dark field, and high angle annular dark field (HAADF) STEM imaging, a probe Cs corrector for atomic resolution scanning transmission imaging (STEM), energy filter and EDX. Samples for transmission electron microscopy were prepared by dispersing tested materials (black powder) in ethanol, placing in

an ultrasonic bath, then putting droplets onto 3 mm copper grids coated with amorphous carbon film and drying in air at room temperature.

3. Results and discussion

3.1. XRD investigations

Fig. 2. shows the XRD pattern for the Pt nanoparticles supported on CNTs. As expected for nanomaterials the obtained spectrum is noisy and difficult to interpret so for the determination of the position of the diffraction peaks curve fitting was performed, what enable to explain shape of the noisy XRD patterns correctly. The combination of one cubic and five Gaussian functions were used for modelling XRD patterns. The best fit (described by the weighted sum of squared residuals value) by Levenberg-Marquardt algorithm was obtained for Gaussian functions presented in Tab. 2. The diffraction peaks in XRD pattern at 46.9 , 53.6 , 81.3 and 99.7° can be assigned to reflections from the (111), (200), (220) and (311) planes of the face-centered-cubic Pt, indicating a good crystallinity of the supported nanoparticles. The broad peaks in the XRD pattern indicate that the platinum nanoparticles are small.

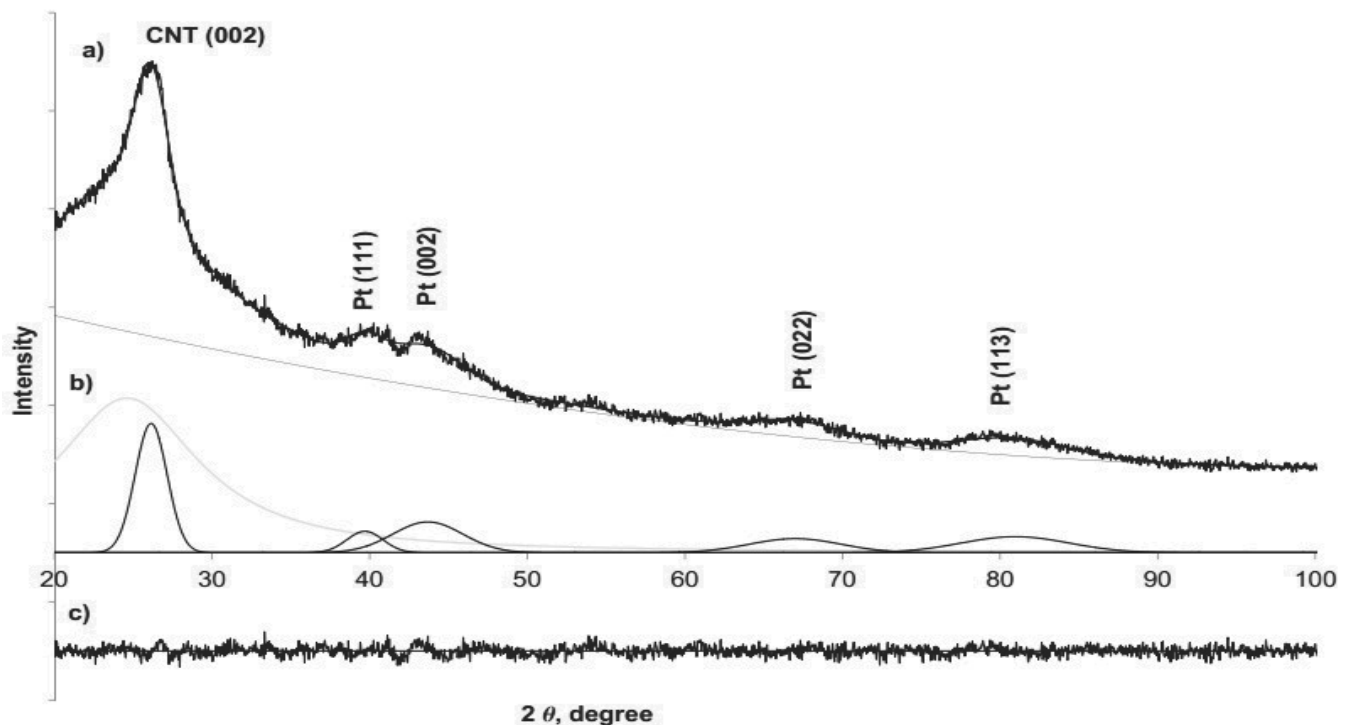


Fig. 2. a) XRD patterns of Pt/CNTs composite; b) Gaussian functions used for modeling XRD patterns by Levenberg-Marquardt algorithm; c) residuals between the calculated fit curve and the observed spectrum

Table 2.
Calculated parameters of Gaussian/Lorentzian functions used for modeling XRD patterns by Levenberg-Marquardt algorithm

Function type	Center, degrees	Area, a.u.	Height, a.u.
Lorentzian	24.63	27200	1579
Gaussian	26.14	3313	1310
Gaussian	39.70	627	218
Gaussian	43.69	1742	313
Gaussian	67.00	1036	143
Gaussian	80.96	1392	163

The average crystallite size of Pt was calculated using the Williamson-Hall's method (Fig. 3). Relationship between $(\beta \cdot \cos\theta)^2$ and $\sin^2\theta$ is linear ($R^2=0.9448$) and make it possible to determine crystallite size. The average crystallite size of platinum nanoparticles was determined as about 9 nm. The diffraction peak at $2\theta=26.2^\circ$ is related to the presence of carbon nanotubes with graphite structure.

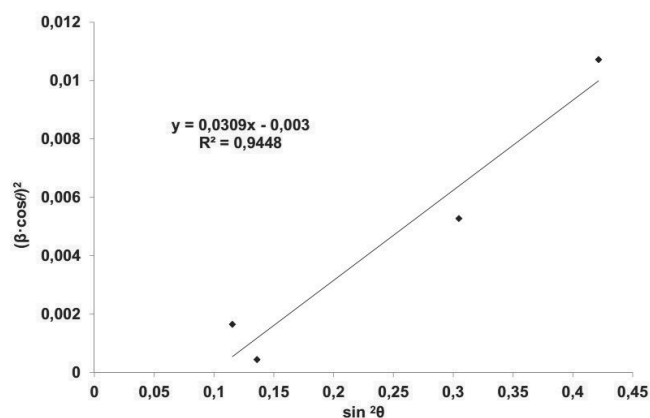


Fig. 3. Relationship between $(\beta \cdot \cos\theta)^2$ and $\sin^2\theta$ for crystallite size determination

Assuming that analysed material is clean - without any admixtures and carbon deposits, one can calculate average distance between graphene layers (d_{002}). Position of the (002) band is connected with an average distance between graphene layers (d_{002}) and can be described as:

$$d_{002} = \frac{\lambda}{2 \sin \theta_{002}}, \quad (4)$$

where λ the wavelength of the X-ray radiation, θ is the Bragg angle of the graphite (002) peak. An average distance between graphene layers determined by powder XRD is 3.62 Å.

3.2. TEM investigations

Fig. 4. presents the image of the raw carbon nanotubes used in the presented work. Obtained result confirm that analysed material is clean - without any admixtures and carbon deposits. Shape ratio is very high, significantly more than 100. Carbon nanotubes are homogenous, very similar in diameter. Average diameter can be estimated as about 10 nm what is clearly visible on the next HRTEM image (Fig. 5). Individual graphene layers are easily visible, typically 3-10 at each nanotube. The intensity variations along line perpendicular to its axis (Fig. 6) demonstrate graphene layer resolution and allow to calculate mean distance between them = 3.52 Å. Obtained value is quite close to value obtained from XRD, but slightly lower. It is a consequence of fact that XRD gives average result while for HRTEM observations better arranged area was chosen.

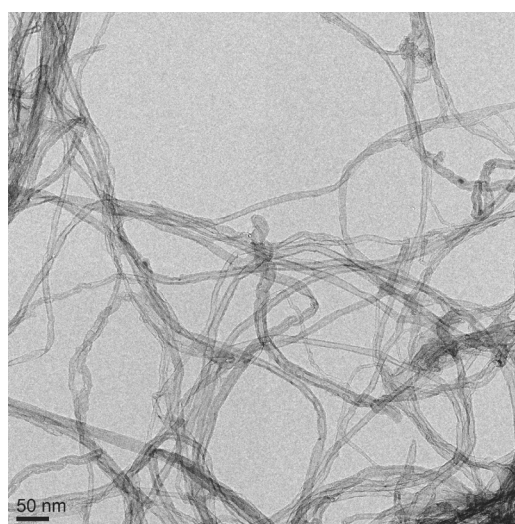


Fig. 4. TEM image of raw carbon nanotubes

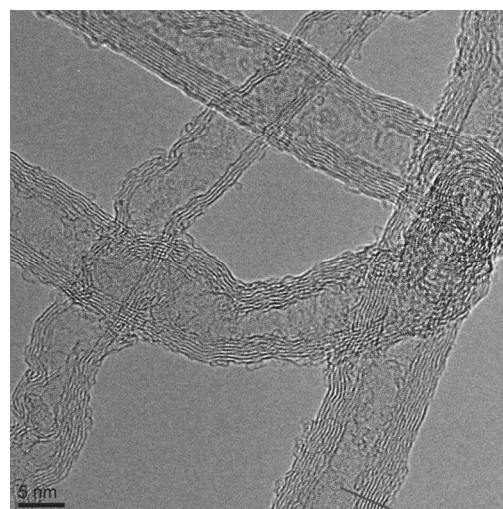


Fig. 5. HRTEM image of raw carbon nanotubes

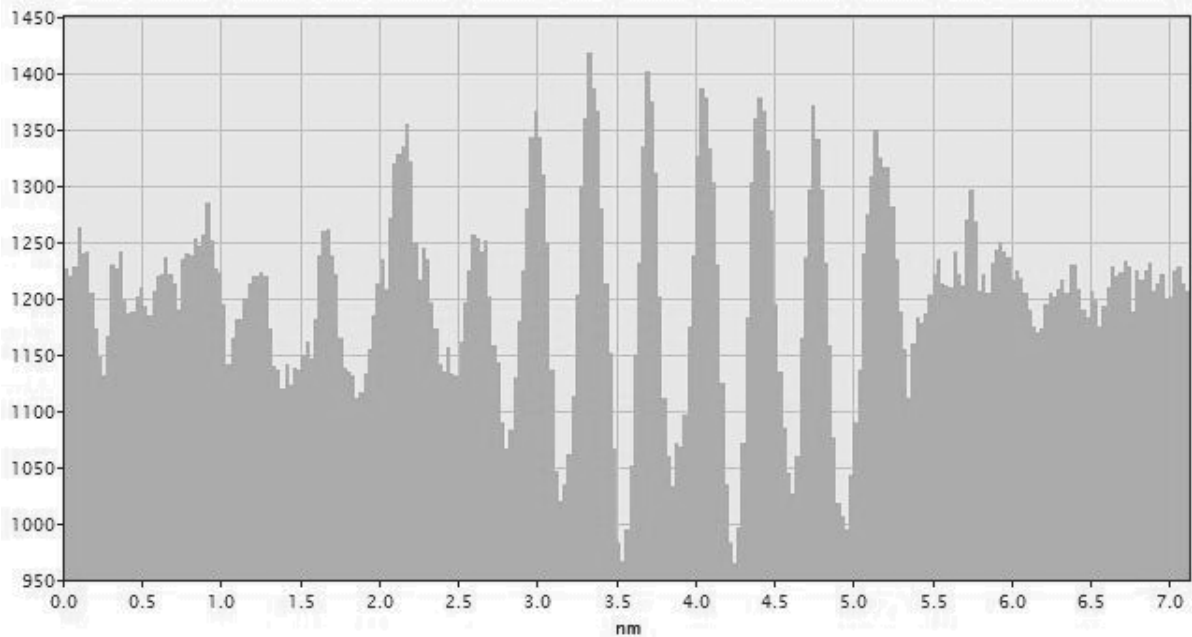


Fig. 6. The intensity variations along the white line in Fig. 5. Determined distance between graphene layer is equal 3.52 \AA

Fig. 7 prove that covering process don't influence significantly on the structure of carbon nanotubes and that their surface was covered by metal nanoparticles.

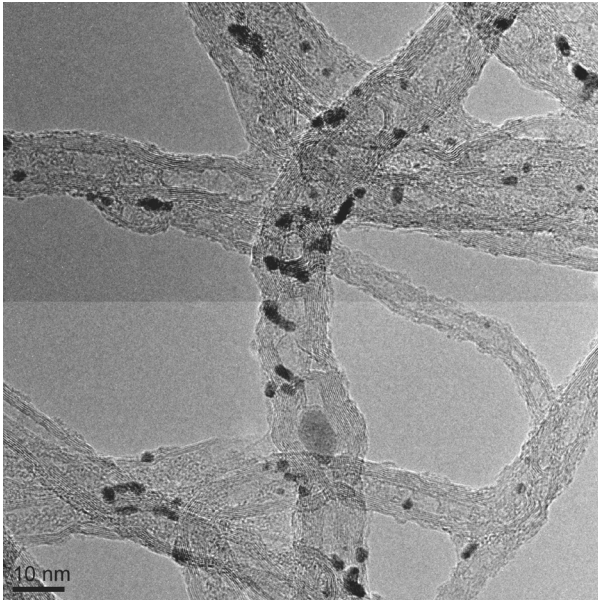


Fig. 7. TEM image of carbon nanotubes covered by platinum nanoparticles

Observed particles appear to have a narrow size distribution, and no free particles were observed in the background of the TEM images, which confirms all formed Pt-NPs were attached to the nanotubes. The surface is coated very densely. It is not conclusive

if they are outside or inside the nanotubes, but the assumption that they are only on the surface appears to be justified. At first approximation their shape is spherical with diameter about 3-4 nm, with a small tendency to agglomerate. Crystal structure is confirmed in Fig. 8 - crystal planes and even atomic column are clearly visible. On the next figure outline of the crystalline shape is present. Crystals are limited by crystalline planes.

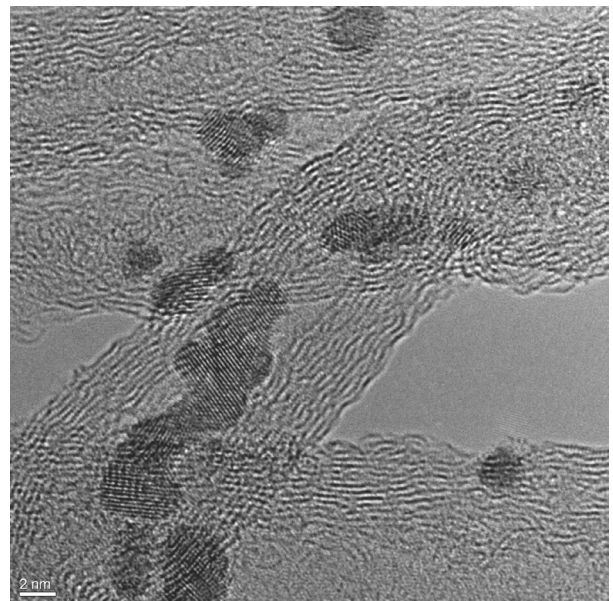


Fig. 8. HRTEM image of carbon nanotubes covered by platinum nanoparticles

As expected it turned out that STEM imaging is very useful at carbon nanotubes covered by platinum nanoparticles characterisation. At that case Pt nanocrystals as having higher atomic number value are visible as light dots (Fig. 9).

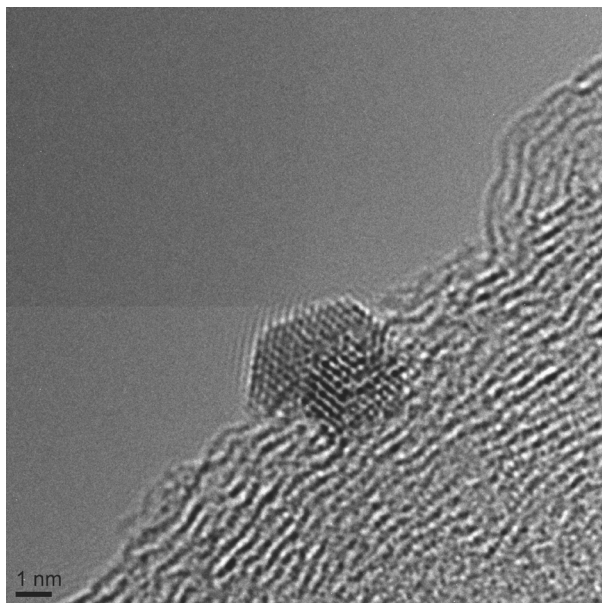


Fig. 9. HRTEM image of the individual platinum nanoparticle

HAADF images (Fig. 10) confirm homogeneous covering of carbon nanotubes by Pt nanoparticles. Large clusters as well as empty fragments were not observed. STEM resolution also make possible to obtain atomic resolution (Fig. 11).

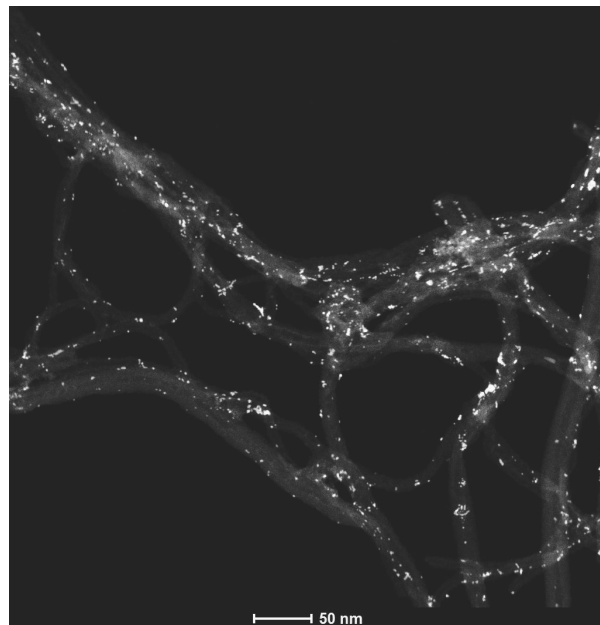


Fig. 10. HAADF image of carbon nanotubes covered by platinum nanoparticles

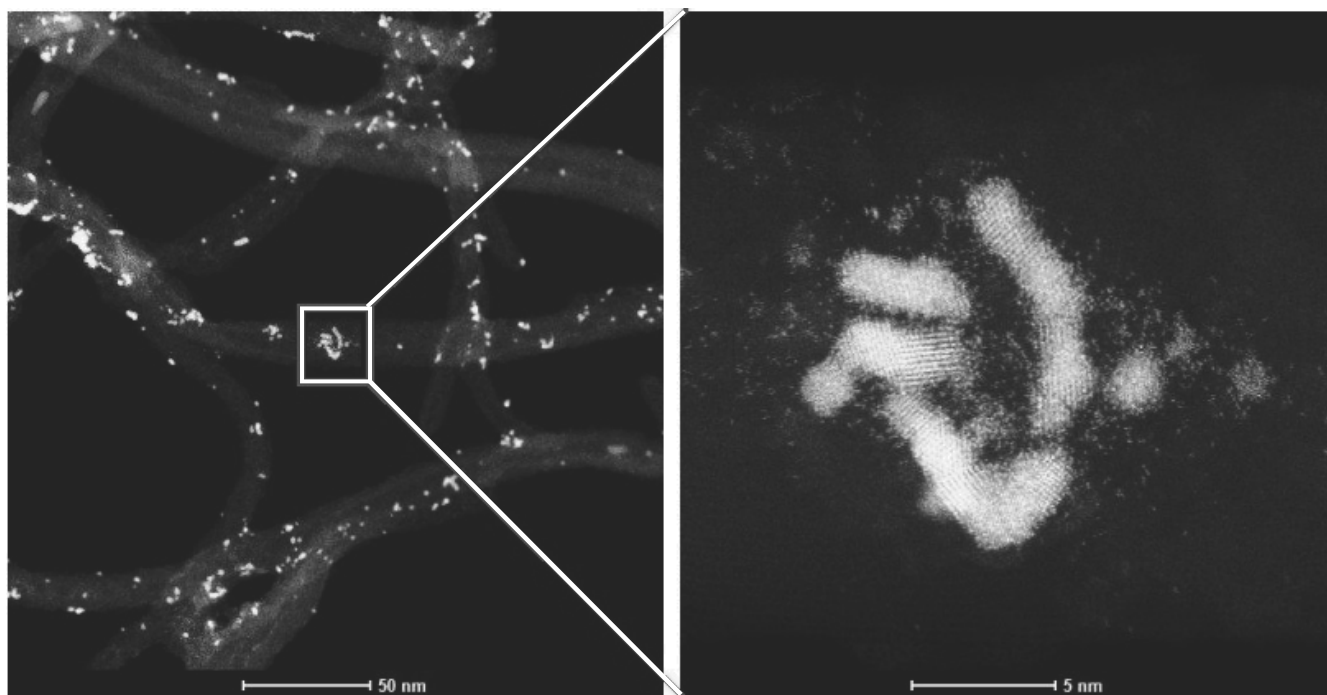


Fig. 11. HAADF images of carbon nanotubes covered by platinum nanoparticles

4. Conclusions and perspectives

Results of characterisation of raw carbon nanotubes as well as carbon nanotubes decorated with platinum nanoparticles were demonstrated in this work. TEM results confirm that CNT were homogeneous and clean, without any admixtures and carbon deposits. Average diameter can be estimated as about 10 nm. An average distance between graphene layers was 3.52 Å. An average XRD result was similar, but slightly higher (3.62 Å). High efficiency of covering carbon nanotubes (without aggregation) by platinum nanoparticles by organic colloidal process was confirmed. Observed particles appear to have a narrow size distribution. Crystal structure was confirmed by TEM images. Crystal shape is polyhedron, limited by crystalline planes, with diameter about 3-4 nm, with small tendency to agglomerate. STEM imaging is very useful at carbon nanotubes covered by platinum nanoparticles characterisation. HAADF images confirm homogeneous covering of carbon nanotubes. Large clusters as well as empty fragments were not observed. STEM resolution also makes it possible to obtain atomic resolution, which is very promising for future defects investigations.

Acknowledgements

The paper has been realised within the framework of the project entitled "Investigation and recognizing a mechanism of changes to the electrical conductivity of carbon nanotubes coated with the nanocrystals of precious metals in the atmosphere of gases obnoxious for the environment" headed by Dr A.D. Dobrzańska-Danikiewicz. That project is funded by Polish National Science Centre in the framework of "OPUS" competitions.

References

- [1] L.A. Dobrzański, M. Pawlyta, A. Krztoń, B. Liszka, K. Labisz, Synthesis and characterization of carbon nanotubes decorated with platinum nanoparticles, *Journal of Achievements in Materials and Manufacturing Engineering*. 39/2 (2010) 184-189.
- [2] B. Liszka, A. Krztoń, M. Pawlyta, Carbon nanomaterials from carbon monoxide using nickel and cobalt catalysts, *Acta Physica Polonica A* 118 (2010) 471-474.
- [3] L.A. Dobrzański, M. Pawlyta, A. Krztoń, B. Liszka, C.W. Tai, W. Kwasny, Synthesis and characterization of carbon nanotubes decorated with gold nanoparticles, *Acta Physica Polonica A* 118 (2010) 483-486.
- [4] L.A. Dobrzański, M. Pawlyta, A. Krztoń, B. Liszka, Carbon nanotubes decorated with platinum nanoparticles as active component of chemical sensors, *Proceedings of the 5th Scientific and Technical Conference Carbon Materials and Polymer Composites, Ustroń-Jaszowiec, 2010*, 16-17.
- [5] M.S. Dresselhaus, G. Dresselhaus, P. Avouris, *Carbon nanotubes: Synthesis, structure, properties and applications*, Springer, 2009.
- [6] R.H. Baughman, A.A. Zakhidov, W.A. De Heer, Carbon nanotubes - the route toward applications, *Science* 297/2 (2002) 787-792.
- [7] M. Endo, M. Strano, P. Ajayan, Potential applications of carbon nanotubes, *Carbon Nanotubes* 111 (2008) 13-61. (http://dx.doi.org/10.1007/978-3-540-72865-8_2).
- [8] Y. Xia, Y. Xiong, B. Lim, S.E. Skrabalak, Shape-controlled synthesis of metal nanocrystals, *Simple chemistry meets complex physics*, *Angewandte Chemie International Edition* 48 (2009) 60-103.
- [9] J. Kong, N.R. Franklin, C. Zhou, M.G. Chapline, S. Peng, K. Cho, H. Dai, Nanotube molecular wires as chemical sensors, *Science* 287/5453 (2000) 622-625.
- [10] W.D. Zhang, W. H. Zhang, Carbon nanotubes as active components for gas sensors, *Journal of Sensors* 2009/160698 (2009) 1-16.
- [11] N. Sinha, J. Ma, J.T.W. Yeow, Carbon nanotube-based sensors, *Journal of Nanoscience and Nanotechnology* 6 (2006) 573-590.
- [12] A. Star, V. Joshi, S. Skarupo, D. Thomas, J.C.P. Gabriel, Gas sensor array based on metal-decorated carbon nanotubes, *The Journal of Physical Chemistry B* 110/42 (2006) 21014-21020.
- [13] S.H.I. Qiao Cui, T.Z. Peng, A novel cholesterol oxidase biosensor based on Pt-nanoparticle/carbon nanotube modified electrode, *Chinese Chemical Letters* 16/8 (2005) 1081-1084.
- [14] H.F. Cui, J.S. Ye, X. Liu, W.D. Zhang, F.S. Sheu, Pt-Pb alloy nanoparticle/carbon nanotube nanocomposite: a strong electrocatalyst for glucose oxidation, *Nanotechnology* 17 (2006) 2334-2339.
- [15] R. Ströbel, J. Garche, P.T. Moseley, L. Jörissen, G. Wolf, Hydrogen storage by carbon materials, *Journal of Power Sources* 159/2 (2006) 781-801.
- [16] M. Hirscher, M. Becher, M. Haluska, F. von Zeppelin, X. Chen, U. Dettlaff-Weglikowska, S. Roth, Are carbon nanostructures an efficient hydrogen storage medium?, *Journal of Alloys and Compounds* 356 (2003) 433-437.
- [17] T. Yildirim, S. Ciraci, Titanium-decorated carbon Nanotubes as a potential high-capacity hydrogen storage medium, *Physical Review Letters* 94/17 (2005) 1-5.
- [18] P. Brown, K. Takechi, P.V. Kamat, Single-walled carbon nanotube scaffolds for dye-sensitized solar cells, *The Journal of Physical Chemistry C* 112/12 (2008) 4776-4782.
- [19] M. Bottini et al., Full-length single-walled carbon nanotubes decorated with streptavidin-conjugated quantum dots as multivalent intracellular fluorescent nanoprobe, *Biomacromolecules* 7/8 (2006) 2259-2263.

- [20] R. Brydson, *Aberation-corrected analytical transmission electron microscopy*, John Wiley & Sons, Ltd, 2011.
- [21] R. Brydson, *Electron energy loss spectroscopy*, Taylor and Francis, 2001.
- [22] <http://www.crystallography.net>.
- [23] www.unipress.waw.pl/fityk/.